Remote Sens. **2014**, *6*, 6688-6708; doi:10.3390/rs6076688

OPEN ACCESS

remote sensing

ISSN 2072-4292

www.mdpi.com/journal/remotesensing

Article

Effect of Bias Correction of Satellite-Rainfall Estimates on Runoff Simulations at the Source of the Upper Blue Nile

Emad Habib [1,*], Alemseged Tamiru Haile [2], Nazmus Sazib [1,†], Yu Zhang [3] and Tom Rientjes [4]

[1] Department of Civil Engineering, University of Louisiana at Lafayette, Lafayette, LA 70504, USA; E-Mail: sazibap25@gmail.com

[2] International Water Management Institute, Nile Basin and East Africa Sub-Regional Office, P.O. Box 5689 Addis Ababa, Ethiopia; E-Mail: A.T.Haile@cgiar.org

[3] NOAA/NWS/OHD, Silver Spring, MD 20910, USA; E-Mail: yu.zhang@noaa.gov

[4] Department of Water Resources, ITC, P.O. Box 6, 7500AA, Enschede, The Netherlands; E-Mail: t.h.m.rientjes@utwente.nl

[†] Current Address: Department of Civil and Environmental Engineering, Utah State University, Logan, UT 84322, USA

[*] Author to whom correspondence should be addressed; E-Mail: habib@louisiana.edu; Tel.: +1-337-482-6513.

Received: 28 March 2014; in revised form: 24 June 2014 / Accepted: 25 June 2014 / Published: 22 July 2014

Abstract: Results of numerous evaluation studies indicated that satellite-rainfall products are contaminated with significant systematic and random errors. Therefore, such products may require refinement and correction before being used for hydrologic applications. In the present study, we explore a rainfall-runoff modeling application using the Climate Prediction Center-MORPHing (CMORPH) satellite rainfall product. The study area is the Gilgel Abbay catchment situated at the source basin of the Upper Blue Nile basin in Ethiopia, Eastern Africa. Rain gauge networks in such area are typically sparse. We examine different bias correction schemes applied locally to the CMORPH product. These schemes vary in the degree to which spatial and temporal variability in the CMORPH bias fields are accounted for. Three schemes are tested: space and time-invariant, time-variant and spatially invariant, and space and time variant. Bias-corrected CMORPH products were used to calibrate and drive the Hydrologiska Byråns Vattenbalansavdelning (HBV) rainfall-runoff model. Applying the space and time-fixed bias correction scheme resulted in slight improvement of the CMORPH-driven runoff simulations, but in some instances

caused deterioration. Accounting for temporal variation in the bias reduced the rainfall bias by up to 50%. Additional improvements were observed when both the spatial and temporal variability in the bias was accounted for. The rainfall bias was found to have a pronounced effect on model calibration. The calibrated model parameters changed significantly when using rainfall input from gauges alone, uncorrected, and bias-corrected CMORPH estimates. Changes of up to 81% were obtained for model parameters controlling the stream flow volume.

Keywords: Center-MORPHing (CMORPH); Gilgel Abbay; satellite rainfall; bias correction; runoff modeling

1. Introduction

Any rainfall-runoff modeling requires accurate rainfall data as model input. However, accurate rainfall information in many world regions is hampered by limitations of ground-based observational networks. Rain gauge networks often have inadequate coverage and density, represent only point scale estimates and suffer from problems relating to data quality and inconsistency [1,2]. Alternative to *in situ* network data are satellite rainfall estimates (SREs), which potentially can be a viable alternative. However, SREs are known to suffer from sampling and estimation inaccuracies, which are manifested in the form of systematic (bias) and random errors [3–7]. Though a number of studies report on usage of SREs for runoff and soil moisture simulations [6,8,9], aspects of accuracy and representativeness of SREs for hydrologic modeling are not well investigated.

In the present study, we focus on bias correction of a particular SRE—the Climate Prediction Center (CPC) Morphing technique (CMORPH; [10]), and the effect of bias correction on hydrologic simulations for the Gilgel Abbay catchment, Lake Tana basin, Ethiopia. CMORPH is considered in this study owing to its relatively high space-time resolutions (30 min, 8 km). In this study CMORPH estimates are accumulated to a daily resolution, which matches the rain gauge sampling interval and the time step of the rainfall-runoff model used herein. A number of studies investigated the accuracy of CMORPH products across a range of space-time scales. Examples include seasonal or daily estimates at 0.25° × 0.25° spatial resolution [11–13], three-hourly estimates at 0.25° × 0.25° [14,15], and one-hourly estimates at 8 km × 8 km [1,5]. Results from these studies suggest that CMORPH estimates have significant systematic biases but also that estimates have random errors. Smith *et al.* [16] stated that CMORPH biases might be due to a diurnal sampling bias, tuning of the instrument or the rainfall algorithm, or unusual surface or atmospheric properties, which the algorithm does not correctly interpret. A Kalman filter approach has been recently adopted by the CMORPH developers to optimally integrate satellite-based estimates with rain gauge observations [17,18]. In the scientific literature, some evidence is presented that CMORPH bias exhibits spatio-temporal variation. For instance, Haile *et al.* [1] show that the total bias and its different components exhibit spatial variation in the Gilgel Abbay catchment, which is also selected for the present study. The authors concluded that over mountain areas CMORPH bias mostly is affected by missed rainfall detection. Particularly for lower elevated areas bias is affected by missed rainfall, false rainfall and differences in hit-rainfall

estimates. For the Nile basin area, Habib *et al.* [11] showed that CMORPH bias (and other SREs) is largely affected by topography and latitude. The same study showed that CMORPH bias in the wet and dry seasons can be quite different.

The aforementioned studies indicate that it is crucial to reduce the systematic and random errors in SREs before products can be used in hydrologic and water resources applications. Methodologies for bias correction are developed in multi-sensor, radar-gauge approaches [19–21] and triggered applications in satellite remote sensing. Examples are on monthly-based bias correction [22], disaggregation of bias at daily scale to hourly scale [23], and merging satellite and gauge data by means of a non-parametric kernel smoother [24]. Vila *et al.* [25] compared five merging schemes: additive bias correction, ratio bias correction, gauge-to-satellite monthly correction factors, and a combined scheme. The authors concluded that the combined scheme, which considers both additive and multiplicative bias, outperformed the others. Other studies of bias-correction to satellite rainfall products are reported in Hong *et al.* [26], Chiang *et al.* [27], Tobin and Bennett [28], and Tian *et al.* [29]. These studies suggest that selection of bias correction scheme should depend on the desired level of accuracy and assumptions to represent spatial and temporal rainfall characteristics. However, selection also depends on the data requirements, computational expenses, and, more importantly, the hydrologic application the bias-adjusted product is used for. Overall, bias-corrected satellite rainfall products are expected to better match station records compared to satellite only products even in complex terrain [30] and as such correction should improve hydrological applications by improved rainfall representation. However, results by hydrological applications are not consistent and require further assessment.

Artan *et al.* [31] showed that negative bias of a satellite rainfall product in rainfall-runoff modeling could result in deterioration of modeling results. They also showed that a hydrologic model requires recalibration when satellite rainfall data is used to replace use of *in-situ* rainfall data. Zeweldi *et al.* [32] reported increased performance of a rainfall-runoff model when the model was calibrated using satellite data than when it was calibrated using rain gauge data. However, calibration could result in parameter values that are unrealistic and beyond limits as the model attempts to compensate for the large errors in rainfall input. Behrangi *et al.* [33] found that bias-adjustment of satellite-based precipitation products is critical and can yield substantial improvement in capturing both the streamflow pattern and magnitude at six-hourly and monthly time scales. Yong *et al.* [34] showed an improvement in the performance of a rainfall-runoff model after applying gauge-based bias correction to satellite-only rainfall products. However, Bitew and Gebremichael [8] reported improved model performance when using a satellite-only product (TRMM 3B42RT) as compared to a satellite-gauge bias corrected product (TRMM 3B42). Such results could be partly attributed to the fairly poor quality and/or lack of spatial representativeness of the sparse gauges that were used for the bias correction.

In the present study, the focus is mainly on analysis of the spatial and temporal variability of bias in CMORPH 30-min, 8 km × 8 km satellite-based rainfall product and on identifying the critical aspects of such variability from a hydrologic perspective in rainfall-runoff modeling. Results of such analyses are of relevance to product users to guide efforts for product adjustment before being used in further applications [35,36] and also for product developers to identify future needs for algorithmic enhancements. The specific objectives of this study are (i) to assess three bias correction schemes to the CMORPH 30-min, 8 km × 8 km product to adjust for spatial and temporal biases; and (ii) to assess

how rainfall-runoff model calibration results are affected when bias-corrected CMORPH data is used instead of uncorrected and *in situ* rainfall data. The area of study is the Gilgel Abbay catchment in Ethiopia. The paper is structured as follows. Section 2 describes the data sets, the bias correction schemes, the hydrologic model, and the calibration approach. Section 3 presents results and discusses the findings and Section 4 concludes on the study.

2. Data and Methods

2.1. Study Setting

The study area is Gilgel Abbay catchment, which is the largest contributor to Lake Tana [37], the source of Upper Blue Nile River in Ethiopia. In the present study, the focus is on the gauged part of Gilgel Abbay for which daily time series of streamflow have been available since the 1970s (Figure 1). This part of the watershed is situated between latitudes of 10°56′N–11°22′N and longitudes of 36°49′E–37°24′E. It covers an area of about 1655 km^2 with predominantly agricultural land cover and with clay to clay-loam as the prevailing soil type. The seasonal rainfall distribution of Gilgel Abbay is affected mainly by the location of the Intertropical Convergence Zone (ITCZ) with a rainy season, which coincides with the summer in the northern hemisphere (June–August). At short time scales (daily and sub-daily), rainfall distribution in this watershed is affected by orographic factors and the presence of Lake Tana [38,39]. The lowlands of Gigel Abbay receive more intense and short lasted rainfall as compared to its highlands [40].

2.2. CMORPH and Local Gauge Data

The satellite-rainfall product used in this study is the National Oceanic and Atmospheric Administration's (NOAA) Climate Prediction Center (CPC) morphing technique (CMORPH) [10]. CMORPH combines rainfall estimates from multiple passive microwave (PMW) sensors, which include the Advanced Microwave Sounding Unit (AMSU-B), the Special Sensor Microwave Imager (SSM/I), the TRMM Microwave Imager (TMI), and the Advanced Microwave Scanning Radiometer—Earth Observing System (AMSR-E), respectively. To fill the time and space gap in the combined PMW based rainfall estimates, the algorithm used cloud motion vectors derived from spatial lag correlation of successive geostationary satellite IR images. These vectors are used to propagate the PMW based rainfall features for time periods between two successive PMW overpasses. The shape and intensity of the rainfall patterns is then morphed through linear interpolation using weights that are obtained from forward advection (previous to most current PMW overpass) and backward advection (most current to previous overpass) of rainfall features. The main advantage of CMORPH is its near real-time global coverage at relatively fine temporal and spatial scales (as fine as 30-min and 8 km × 8 km), which makes it a desirable candidate for hydrologic applications. In the current analysis, the 30-min, 8 km × 8 km CMORPH estimates are aggregated to daily time step to be consistent with rain gauge observation interval. In addition, streamflow time series are at daily time interval so aggregation results in optimal use of available satellite data to represent and to correct rainfall in respective time and space domains for stream flow modeling. Based on availability of rain gauge and

streamflow data in the watershed, the current analysis period covers two years from January 2003 to December 2004.

Figure 1. Study site showing the location of the Gilgel Abbay catchment and its eight sub-catchments within the Nile Basin. The locations of the ten (10) rain gauge stations and the streamflow gauge are indicated. Note that the unit of terrain elevation is meters. (**a**) Geographic location of study area; (**b**) Terrain elevation and rain gauge stations.

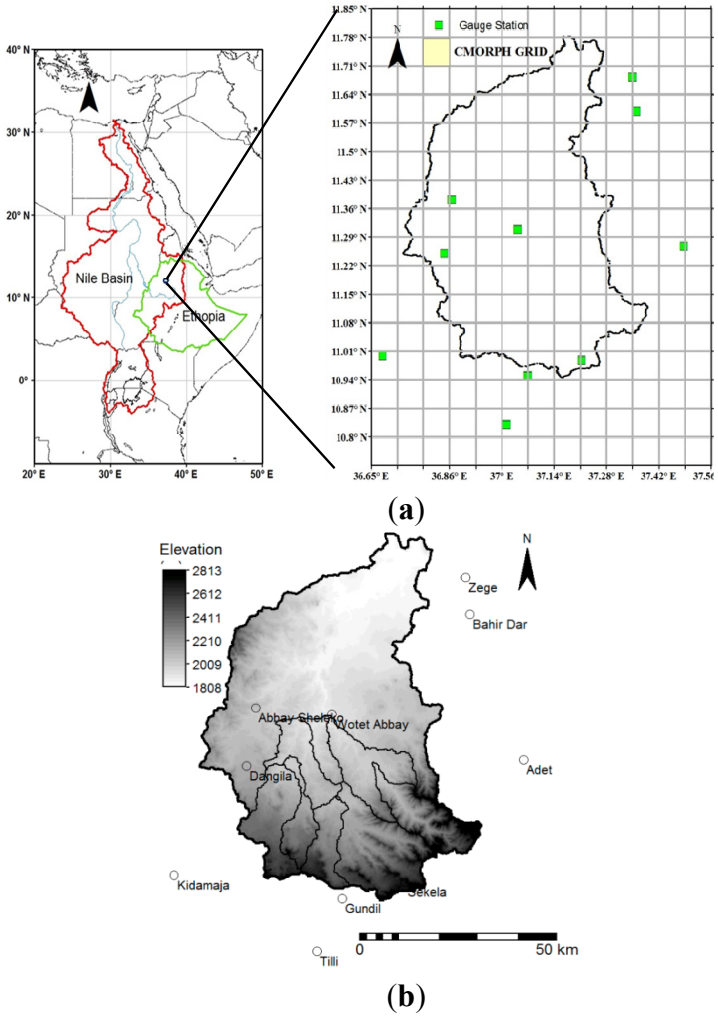

Data is obtained from 10 rain gauges in the watershed (Figure 1) which are operated by the Ethiopian Meteorological Agency (EMA). Daily rainfall from these gauges has been evaluated and used in [37,41–43] and serve as reference to evaluate satellite rainfall estimates. For the study period, the average annual rainfall over Gilgel Abbay was about 1700 mm. The average daily rainfall rate exceeded 10 mm/day for 20% of the time and reached as high as 35 mm/day. The gauge network (Figure 1) is sparse and stations are unevenly distributed over the watershed. As a result, the "true" or real world rainfall distribution may not be well represented by the network, as rainfall varies over the area following topographic variation [1,38,39].

Meteorological observations at three stations in the watershed (Dangila, Adet, and Bahir Dar; Figure 1) were used to estimate monthly potential evapotranspiration (PET) using the Penman-Montheith method [44], which were then used as input to the hydrologic model.

Streamflow daily data is available for the upper part of Gilgel Abbay, which is gauged at Wotet Abbay, a small town near Bahir Dar. Consistency of streamflow daily time series was checked by visual inspection of concurrent rainfall and streamflow plots. We noticed that the baseflow record showed an abrupt increase in late 2005. Local people near the gauging site stated that the gauging station was moved by hundreds of meters downstream of the original site towards the end of 2005 due to road construction. However, this was not confirmed by officials in the Ministry of Water Energy. As a result we limited our analysis period to 2003 and 2004 for which CMORPH data is available and for which we have confidence in the quality of stream flow data.

2.3. Bias Formulation and Estimation

Satellite-based rainfall estimates exhibit large systematic and random errors. The systematic errors (*i.e.*, bias) persist when the estimates are aggregated over time and, hence, may cause large uncertainties in hydrologic modeling. In addition, models could augment or suppress rainfall biases to larger or smaller streamflow based on the response mode of the model. Therefore, bias in rainfall products should be assessed and corrected before satellite rainfall products can be used in hydrologic applications.

In the current study, we estimate and correct the bias in CMORPH estimates as follows. For a selected day (d) and gauge (i), the multiplicative daily bias factor (BF) at a certain CMORPH pixel with a collocated gauge can be formulated as follows Equation (1):

$$BF_{TSV} = \frac{\sum_{t=d}^{t=d-l} S(i,t)}{\sum_{t=d}^{t=d-l} G(i,t)} \quad (1)$$

where G and S represent daily gauge and CMORPH rainfall estimates, respectively, i refers to gauge location, t refers to a Julian day number; and l is length of a time window for bias calculation. The subscript "*TSV*" stands for "Time-Space Variable" since the bias in this formulation is estimated for a particular location and a particular day. Based on some preliminary analysis by the authors on rainfall distributions in the study area, a fixed time window of l = 7 days was selected to allow for adequate rainfall accumulation for bias calculation while still accounting for temporal variability in BF. The BF factor was calculated for a certain day only when a minimum of five rainy days were recorded within the preceding seven-day window with a minimum rainfall accumulation depth of 5 mm, otherwise no bias is estimated (*i.e.*, assigned a value of 1). We chose five rainy days with minimum accumulation depth of 5 mm to ensure stability of the bias factors and avoid exaggerated values as a result of dividing large satellite estimates by small gauge values. We evaluated sensitivity of BF to different window lengths of 3, 7, and 10 days. We noticed that BF shows relatively lower sensitive during the wet season compared to the dry season. In the wet season, BF shows high variation and becomes highly erratic when the window length is reduced to three days as a result of small accumulation period. In the wet season, BF exceeds 2.0 for a three-day window length but is mostly well below 2.0 for a seven- and 10-day window length.

It is noted that Equation (1) ignores errors introduced by using a single gauge to represent rainfall amounts at the scale of the CMORPH pixel. Haile *et al.* [1] showed that the error variance of the gauge representativeness error in Gilgel Abbay could contribute as much as 30%–52% to the total variance of CMORPH-gauge rainfall hourly differences. Using the current dataset, we found that the spatial correlation of rainfall in the study area, at 8 km separation distance, increases from 0.55 at a daily scale

to 0.91 for a seven-day accumulation scale. Therefore, it is reasonable to assume that the gauge representativeness error will be much smaller at a seven-day time window than that of the hourly base, and, thus, we proceed with using single-gauge observations as a reference for the bias estimation using Equation (1).

2.4. Schemes for Bias Correction

In the current analysis we test three schemes for bias correction:

(i) The first one allows for correcting the bias at a pixel based (*i.e.*, space variable) and at a daily scale (*i.e.*, time varying), and is based on the using the BF_{TSV} factor estimated from Equation (1). To apply a correction that accounts for spatial and temporal variability in the CMORPH bias, the pixel-based daily BF_{TSV} factors were spatially interpolated using the inverse distance weight (IDW) method to yield a spatial and temporally varying field of *BFs* that cover the entire study area. We followed the approach of Haile *et al.* (2009) [38] in the same study area who showed good interpolation results by IWD. The CMOPRH daily rainfall fields were then multiplied by the BF_{TSV} bias fields for the respective time windows to result in a new set of CMORPH estimates that as such are bias-corrected in a temporally and spatially varying scheme. This procedure is similar to the local-bias correction algorithm developed by Seo and Breidenbach [19], which is adopted in the operational version of the National Weather System-Multisensor Precipitation Estimation (NWS-MPE) system. The use of Equation (1) applies a bias correction factor that varies in space and time domains. We refer to this formulation as time and space variant (TSV) bias correction. To assess the implications for ignoring or for accounting of variability of bias, two more bias estimation and correction schemes were tested:

(ii) Time and space fixed (TSF) bias correction: in this formulation the bias is obtained by using gauge and CMORPH estimates over the entire domain and over the total duration of the sample Equation (2):

$$BF_{TSF} = \frac{\sum_{t=1}^{t=T}\sum_{i=1}^{i=n} S(i,t)}{\sum_{t=1}^{t=T}\sum_{i=1}^{i=n} G(i,t)} \quad (2)$$

where n is the total number of gauges within the entire domain of the study and T is the full duration of the study period. The bias correction in this case is applied by multiplying the CMORPH estimates by the bias factor, BF_{TSF}, to result in a new set of CMORPH estimates that are bias-corrected in a spatially and temporally-lumped scheme.

(iii) Time variable (TV) bias correction: in this formulation the *BF* is spatially lumped over the entire domain but is still estimated for each daily time step Equation (3):

$$BF_{TV} = \frac{\sum_{t=d}^{t=d-l}\sum_{i=1}^{i=n} S(i,t)}{\sum_{t=d}^{t=d-l}\sum_{i=1}^{i=n} G(i,t)} \quad (3)$$

The bias correction in this case is applied by multiplying each daily CMORPH field by the daily bias factor, BF_{TV}, to result in a new set of CMORPH estimates that are bias-corrected in a spatially-lumped but temporally-varying scheme.

2.5. Hydrologiska Byråns Vattenbalansavdelning (*HBV-96*) *Hydrologic Model*

In the present study, the Hydrologiska Byråns Vattenbalansavdelning (HBV-96) rainfall-runoff model [45] is used to perform the rainfall-runoff analysis using rainfall estimates by the three correction schemes. The HBV-96 model has been extensively evaluated for different regions on the globe [46–50] including Gilgel Abbay catchment [37,41,43]. HBV-96 can be classified as a conceptual model that relies on water balance equations to simulate runoff and mass exchanges across a set of surface and subsurface zones. Inputs to the model include rainfall, temperature, potential evapotranspiration, and percentage of forested and non-forested catchment areas.

The storage based HBV-96 has four routines that include (i) a precipitation accounting routine; (ii) a soil moisture routine; (iii) a quick runoff routine; and (iv) a base flow routine. The approach is characterised by three stores, which are the soil moisture reservoir, the upper zone store and the lower zone store. From the upper zone store quick runoff is simulated from the lower zone store base flow runoff is simulated. Routing of streamflow is optional and can be de-activated in model simulations. The precipitation accounting routine partitions precipitation into rainfall and snow based on a threshold value (TT). Precipitation is in the form of snow in case the actual temperature (T) is lower than TT. In the Gilgel Abbay area, the temperature is much higher than common values for TT and, as such, precipitation only is in the form of rainfall.

The soil moisture routine controls the formation of direct and indirect runoff. Direct runoff occurs when the simulated soil moisture (*SM*) in the soil moisture reservoir exceeds the maximum storage capacity as represented by field capacity (FC). Otherwise, rainfall infiltrates (*IN*) the soil moisture reservoir to add to the actual storage and to add to the flow of water to the upper zone store (indirect runoff).

Indirect runoff (*R*) is defined as follows:

$$R = IN\left(\frac{SM}{FC}\right)^{BETA} \tag{4}$$

This equation indicates that indirect runoff increases with increasing soil moisture storage (*SM*) but it reduces to zero when infiltration ceases. *BETA* is a parameter accounting for the non-linearity of indirect runoff from the soil layer.

Evapotranspiration losses are calculated from the soil moisture reservoir. Actual evapotranspiration (E_a) is highest (*i.e.*, reaches its potential value (E_p)) when *SM* reaches or exceeds a certain ratio of *FC*. The ratio, denoted as *LP*, is used as a calibration parameter. Otherwise, E_a declines linearly as a function of soil moisture deficit represented by *SM/FC*:

$$E_a = E_p \qquad if\ SM \geq (LP \cdot FC) \tag{5}$$

$$E_a = \frac{SM}{LP \cdot FC} \cdot E_p \qquad if\ SM < (LP \cdot FC) \tag{6}$$

Percolation (*PERC*) to the lower zone store occurs when water is available in the upper zone store. *PERC* is treated as a time-invariant process with a fixed value throughout the simulation period. Capillary transport is estimated as a function of soil moisture deficit (*FC*-*SM*) and a maximum value for capillary flow (*CFLUX*):

$$C_f = CFLUX \cdot \left(\frac{FC - SM}{FC} \right) \tag{7}$$

Quick runoff (Q_q) and slow (base) flow (Q_s) are defined as follows:

$$Q_q = K_q UZ^{(1+ALPHA)} \tag{8}$$

$$Q_s = K_s LZ \tag{9}$$

where *UZ* is the actual storage in the upper zone store, *ALFA* is a measure for the non-linearity of flow, K_q is a recession coefficient for quick runoff, *LZ* is the actual storage in the lower zone store and K_s is a recession coefficient for base flow. According to this formulation, the model has 8 parameters that can be used for model optimization and calibration, namely: *FC*, *BETA*, *LP*, *ALPHA*, K_q, K_s, *PERC*, and *CFLUX*.

Considering the large catchment area and significant topographic variation, and to make use of the spatially distributed data from CMORPH, the catchment has been partitioned in eight sub-catchments (Figure 1). The eight sub-catchments have size of 76, 121, 150, 165, 240, 242, 245, and 414 km^2.

2.6. Model Calibration and Evaluation

The model was calibrated using four sets of rainfall data based on gauge observations, and three variants of bias corrected CMORPH estimates. In both cases, rainfall data were aggregated from their original spatial resolutions (gauge-point, or CMORPH pixel) to the scale of each sub-catchment.

The following two metrics were used to assess performance of the HBV-96 rainfall-runoff model: Nash-Sutcliffe (*NS*) efficiency, which provides a measure of random differences between simulated and observed streamflows, and Q_{Bias}, which measures systematic differences (bias) in the simulated streamflow volumes:

$$NS = 1 - \frac{\sum_{i=1}^{n} (Q_{sim,i} - Q_{obs,i})^2}{\sum_{i=1}^{n} (Q_{obs,i} - \overline{Q_{obs}})^2} \tag{10}$$

$$Q_{Bias} = \left(\frac{\sum_{i=1}^{n} Q_{sim,i}}{\sum_{i=1}^{n} Q_{obs,i}} \right) \tag{11}$$

where Q_{sim} and Q_{obs} represent simulated and observed daily flows, respectively, at a certain day *i*, and *n* represents the number of days in the sample. The over-bar symbol denotes the mean statistical operation. The values of *NS*, which is dimensionless, can range between $-\infty$ and 1, where a value of 1 indicates a perfect fit. Similarly, a Q_{Bias} value of 1 reflects bias-free streamflow simulations whereas streamflow overestimation and underestimation are reflected by bias values that are larger or smaller than 1, respectively.

A Monte-Carlo procedure was used to calibrate the HBV-96 model. In this procedure, prior ranges of the eight calibration parameters are selected based on the parameter value ranges specified

by Rientjes *et al.* [37] who applied the HBV-96 model in a regionalization study in the (entire) Lake Tana basin area. In that particular study 60,000 parameters sets are generated randomly assuming a uniform distribution of parameter values within the specified, posterior, value ranges. The HBV-96 model was run for each parameters set and the corresponding objective function values (*NS* and Q_{Bias}) are calculated. Following Rientjes *et al.* [37], the optimum parameters set is selected as the average value of the 25 parameter sets that are ranked highest in terms of the *NS* values. It is noted that a similar approach is followed in this study when calibrating the model in case CMORPH rainfall data is used as model input.

3. Results

3.1. Evaluation of CMORPH Estimates

Before presenting the results of the different bias correction schemes, we first examine the temporal and spatial variability in the CMORPH bias field, as reflected by BF_{TSV} (Figure 2). The lowest, highest and mean values of BF_{TSV} for a seven-day moving window are shown in the figure. These values are summarized based on BF_{TSV} values calculated at the ten rain gauge stations within the study area. For each calendar day the minimum, maximum and mean are shown for the ensemble of network stations. The difference between the lowest and highest values shows the extent of the variation of the bias across the 10 stations in the study area. The mean values show pronounced seasonal variations and have different patterns throughout the two years. In general, CMORPH reports smaller rainfall amounts than gauge observations from mid-June to mid-August 2003, but reports larger rainfall amounts towards the end of the rainy season of 2003. This pattern is not shown in 2004, where positive and negative biases in CMORPH show lower variation in time. Overall, these results indicate that the bias in the CMORPH product exhibits pronounced variability in space and time over the study area. Possibly, this could be related to variations in rain generation mechanisms [11] but further investigations are needed for confirmation.

3.2. Results on Rainfall Bias Correction

To examine the implications of space and time variability presented above (Figure 2), we applied the three bias correction schemes described above (Equation (1)), time-space fixed (TSF), time variable (TV), and time-space variable (TSV), to the CMORPH product. We first assess how the different bias correction schemes impact the catchment-average rainfall at a monthly scale. Table 1 shows a summary of the ratios of CMORPH monthly catchment-average rainfall amounts (before and after correction) to the corresponding gauge amounts. Without bias correction, CMORPH mostly underestimated monthly rainfall by up to 37%. In 2003, the deviation of CMORPH during the wettest months (June-August) is reduced when TSF, TV, or TSV corrections are used. TSV correction shows noticeable change (up to 0.19) than TSF correction (only 0.01) in July 2003. In 2004, TSF correction leads to deterioration of the monthly agreement probably since their temporal variation is too pronounced to be ignored. The importance of accounting for temporal variation in CMORPH bias is illustrated again by the fact that TV and TSV corrections reduced the bias in 2004 by up to 0.07 and 0.07–0.14, respectively.

Figure 2. Mean, minimum and maximum of CMORPH daily bias factors (BF_{TSV}, Equation (1)) evaluated for the ensemble of ten network stations.

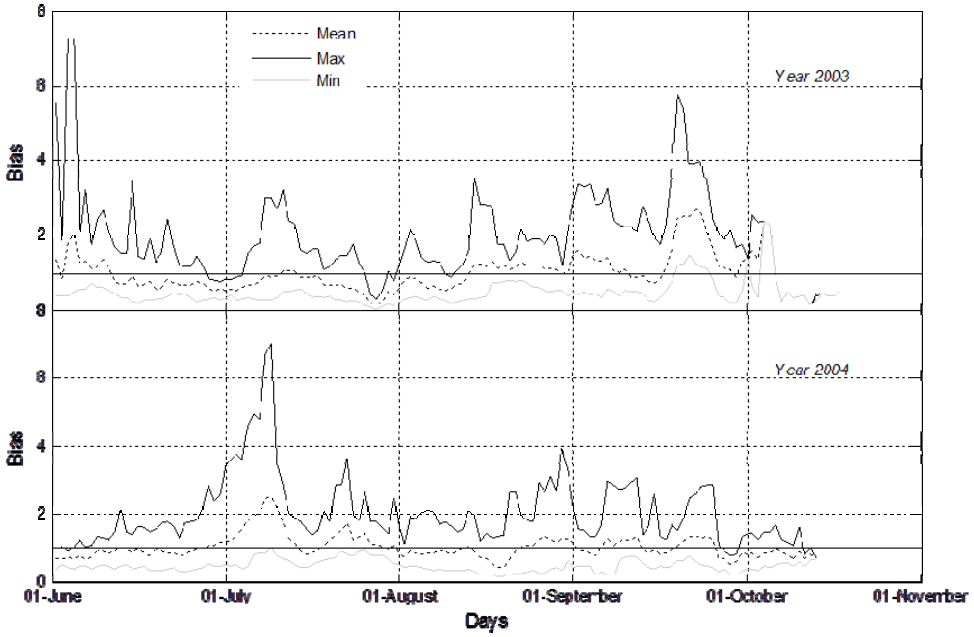

Table 1. Ratios of monthly rainfall amounts of Climate Prediction Center-MORPHing (CMORPH) (without and with three bias correction schemes) to the corresponding gauge amounts.

Year	Rainfall Product	June	July	August	September	October
2003	*CMORPH*	0.69	0.63	0.88	1.25	0.74
	CMORPH TSF	0.71	0.64	0.9	1.28	0.76
	CMORPH TV	0.74	0.82	0.94	0.9	0.63
	CMORPH TSV	0.87	0.81	0.99	0.95	0.63
2004	*CMORPH*	0.83	1.15	0.8	0.99	0.84
	CMORPH TSF	0.79	1.09	0.76	0.94	0.8
	CMORPH TV	0.9	0.87	0.87	0.93	0.93
	CMORPH TSV	0.95	0.86	0.87	0.96	0.98

3.3. Model Parameter Optimization Using Different Rainfall Inputs

We calibrated the HBV-96 model using gauge and CMORPH rainfall inputs for the year 2003–2004 (Table 2). Calibration based on the rain gauge network data serves as a reference for further assessments on effectiveness of bias-correction to the CMORPH estimates. The model was recalibrated using the satellite rainfall fields to examine how the model parameters are affected by bias in the rainfall input. In theory, each rainfall input represents a different model forcing and may result in different parameter values and model performance level as measured by *NS* and *Qbias*. Independent calibration of the HBV-96 model for different rainfall inputs resulted in satisfactory model performance (NS = ~0.8 and Q_{Bias} = ~0.9). All optimum parameter values obtained using the correction schemes are within the allowable value ranges. The values of the optimized model parameters are inter-compared and percent change of each parameter value is shown with respect to the reference case. To allow

comparison of parameter values over a common scale, changes are calculated after normalizing the parameter values using their allowable minimum and maximum values, which are set equal for all simulations. We note that the results of parameter optimization are affected by the rainfall input as shown by the percentage errors in Table 2. In particular, parameters (*FC*, *Beta* and *LP*) which control the volume of the simulated hydrograph showed large changes of up to 81% compared to the parameters using the reference gauge data sets. There is also a significant change in the quick recession coefficient (K_q), whereas those that control groundwater contributions (K_s, *PERC* and *CFLUX*) are less affected.

Table 2. Calibrated values of the Hydrologiska Byråns Vattenbalansavdelning (HBV) model parameters using gauge and bias corrected CMORPH. Numbers in brackets represent percent changes in each parameter value (after normalizing with the allowable minimum and maximum range) with respect to the gauge-driven reference case. The last two rows show the *NS* and Q_{Bias} values.

Parameter	Unit	Minimum	Maximum	Gauge	CMORPH with Bias Correction		
					Time-Space Fixed (TSF)	Space Fixed and Time Variable (TV)	Time-Space Variable (TSV)
FC	mm	100	800	373	186 (−68)	177 (−72)	185 (−69)
BETA	--	1	4	1.351	1.599 (71)	1.562 (60)	1.625 (78)
LP	--	0.1	1	0.544	0.888 (77)	0.905 (81)	0.775 (52)
ALPHA	--	0.1	3	0.271	0.242 (−17)	0.236 (−20)	0.269 (−1)
K_q	day^{-1}	0.0005	0.15	0.073	0.035 (−52)	0.050 (−32)	0.038 (−48)
K_s	day^{-1}	0.0005	0.15	0.087	0.086 (−1)	0.083 (−5)	0.074 (−15)
PERC	$mm \cdot day^{-1}$	0.1	2.5	1.348	1.422 (6)	1.208 (−11)	1.339 (−1)
CFLUX	mm	0.0005	2.0	0.886	0.898 (1)	0.805 (−9)	0.892 (1)
NS	--	--	--	0.8256	0.703	0.8038	0.8177
Q_{Bias}	--	--	--	0.995	0.982	0.988	0.982

3.4. Effects of Rainfall Bias Corrections on Streamflow Simulations

Next, we applied the calibrated parameter set of the reference case to simulate streamflow using the uncorrected and bias-corrected CMORPH rainfall estimates. We chose to use the reference set of parameters to in all model simulations (gauge and CMORPH) to isolate the effect of rainfall bias from other sources of model uncertainty (e.g., parameter uncertainty). Figure 3 shows streamflow hydrographs for the reference case and for uncorrected CMORPH estimates. At the beginning and middle of the 2003 wet season, differences between CMORPH gauge rainfall amounts are negative for most of the time. For this reason, lower streamflow discharges are simulated. Towards the end of the rainy season of 2003, positive rainfall differences start to appear but this did not cause higher streamflow discharges than observed. It appears that the excess rainfall was stored in the different model stores instead of generating runoff. Relatively large positive differences in rainfall dominate towards the beginning of the wet season of 2004. This rainfall difference resulted in higher streamflow simulations than observed. The rainfall difference becomes negative throughout August 2004, but it did not produce negative streamflow biases, as the model stores had the excess rainwater from previous time

steps stored. Overall, these results indicate that CMORPH bias propagates into model simulations. The bias correction affects moisture conditions which yielded lower (excess) runoff than observed.

Figure 3. (**a**) Comparison of daily catchment-average gauge and uncorrected CMORPH rainfall. (**b**) differences in daily rainfall estimates between gauge and CMORPH. (**c**) and (**d**) observed and simulated stream flow hydrographs for the year June 2003–December 2004 based on rainfall inputs from gauges and uncorrected CMORPH.

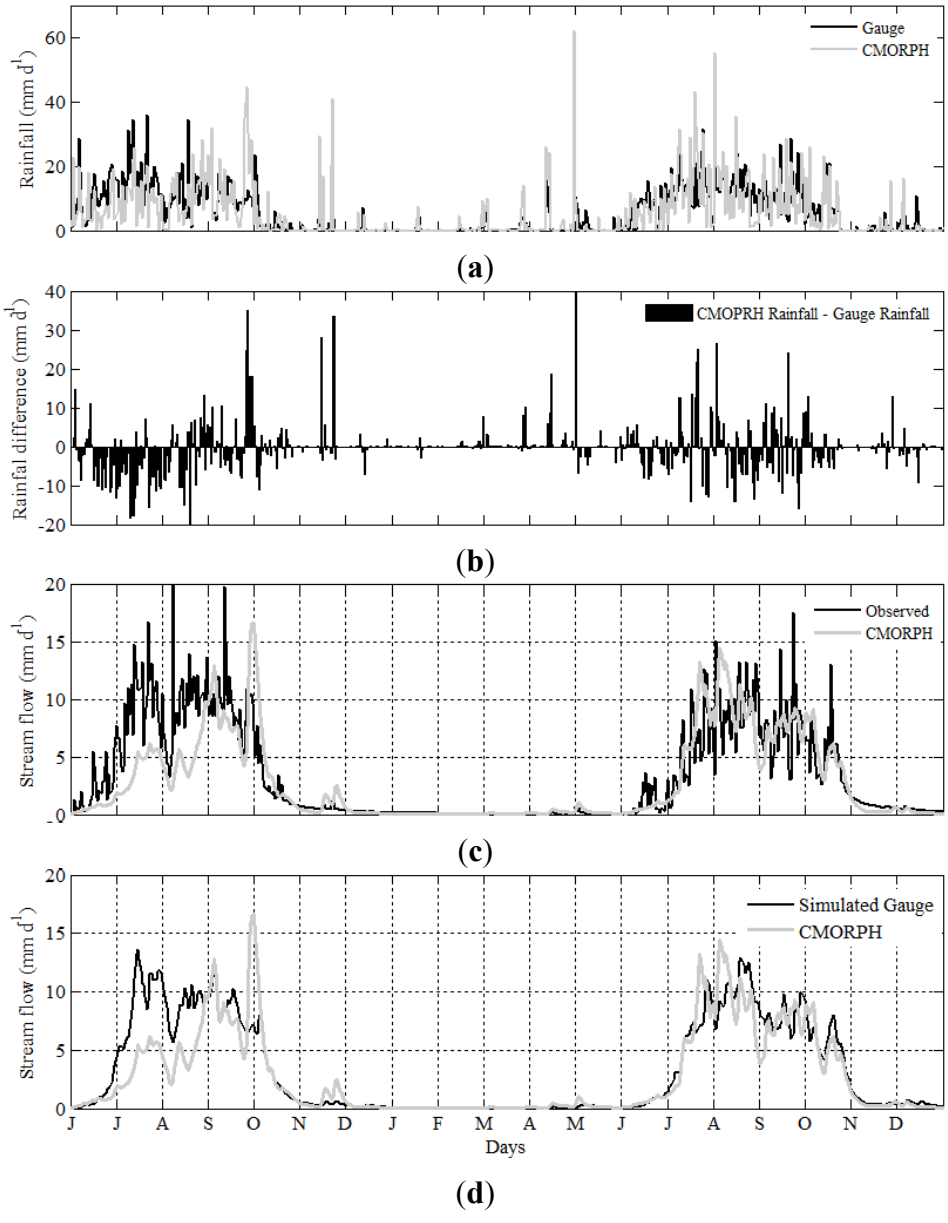

Next, we evaluated the effect of bias correction in CMORPH on HBV-96 model simulations (Figure 4). Here we show the streamflow hydrograph that is simulated using TSV bias-corrected CMORPH data, which produced the best result. Despite the applied bias correction, there are large differences (>10 mm·d^{-1}) between catchment-average daily rainfall estimates obtained from TSV and gauges. However, it is apparent that the large CMORPH bias in 2003 was substantially reduced. As a result, the patterns and volumes of the observed hydrographs were better captured when using the bias-corrected CMORPH estimates than the uncorrected ones. Some observed peak flows were better

captured as a result of correcting for the rainfall bias. The improvements are particularly substantial for the 2003 hydrographs where the uncorrected CMORPH had large negative bias. We note that use of bias corrected rainfall data has some advantages over gauge only data; however, some aspects of observed hydrograph were better captured by using gauge only data (e.g., the second half of July 2003). The simulated hydrographs based on both rainfall inputs show smaller fluctuation than the observed hydrograph. Such mismatches could be caused by deficiencies in the HBV-96 model structure, poor rainfall representation by the low density of the rain gauge network, or errors in streamflow observations, among others.

Figure 4. (**a**) Comparison of daily catchment-average gauge rainfall and the corresponding TSV bias-corrected CMORPH. (**b**) differences in rainfall estimates between gauge and TSV bias-corrected CMORPH. (**c**) and (**d**) observed and simulated stream flow hydrographs for the year June 2003–December 2004 based on rainfall inputs from gauges and TSV bias-corrected CMORPH.

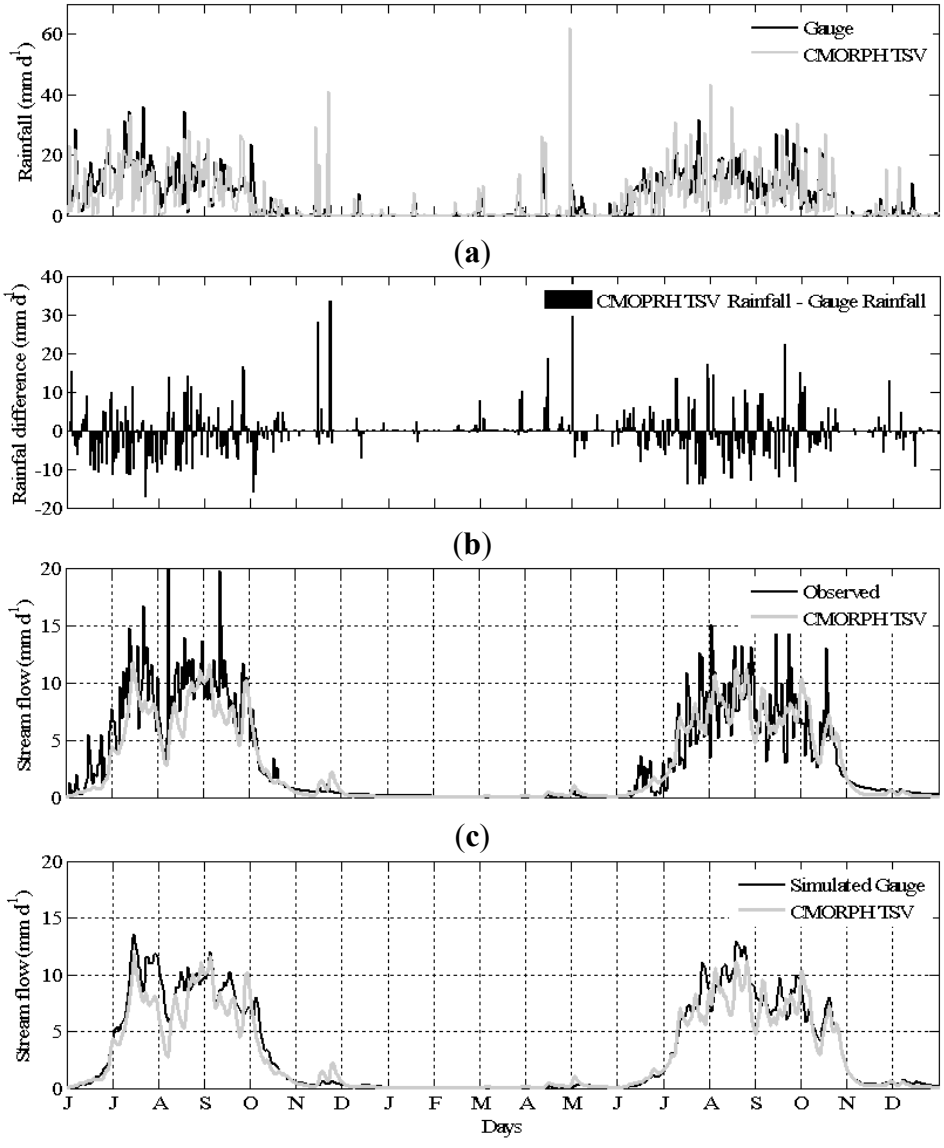

Next, we quantify the propagation of CMORPH rainfall biases in model simulations (Table 3). To separate the effect of rainfall errors from effects of model parameter uncertainty on model performance, gauge-based model simulations served as reference to compare the model performance objective functions. In June–August 2003, CMORPH rainfall amounts are smaller than those from gauges by −18% (CMORPH bias ratio = 0.82), which causes difference in streamflow volume of −27% (streamflow bias = 0.73) and increased for the same period of 2004 (from −5% to −27%). This rainfall-to-streamflow bias amplification persists for all of the CMORPH rainfall inputs but its extent became smaller when the temporal variability of the bias is considered (*i.e.*, when using time-varying bias correction, BF_{TSV}). For example, for CMORPH TSV rainfall input, the bias increased from −13% to only −17% in 2003 while it increased from −8% to 20% in 2004. The observed changes of rainfall-to-streamflow biases are probably due to the non-linearity in the rainfall-runoff relation and subsequent runoff generation in the HBV-96 model. For instance, small bias in rainfall input can propagate to result in larger streamflow bias when the catchment is wet than when it is dry.

Table 3. Ratios of catchment-average seasonal rainfall amounts of CMORPH (without and with three bias correction schemes) to the corresponding gauge amounts. The corresponding values for streamflow biases (Q_{Bias}) are also presented. The *NS* efficiency values for the streamflow simulations are shown between brackets.

Year	Performance Measure	CMORPH	CMORPH (TSF)	CMORPH (TV)	CMORPH (TSV)
June–October 2003	*Rainfall Ratio*	0.818	0.819	0.806	0.869
	Streamflow Q_{Bias}	0.734 (*0.19*)	0.762 (*0.21*)	0.764 (*0.71*)	0.831 (*0.79*)
June–October 2004	*Rainfall Ratio*	0.947	0.904	0.898	0.917
	Streamflow Q_{Bias}	0.726 (*0.73*)	0.727 (*0.73*)	0.792 (*0.79*)	0.804 (*0.80*)

Streamflow bias, Q_{Bias} (Equation (9)), obtained using the uncorrected as well as the bias-corrected CMORPH rainfall inputs are shown in Figure 5 (see also Table 3). As compared to gauge-based simulations, the uncorrected and bias-corrected CMORPH data resulted in consistently smaller streamflow in the rainy season (June–August) of 2003 but larger streamflow towards the end of the rainy season. Note that this pattern has some resemblance to that of the rainfall biases (Figure 2). However, the temporal pattern of the streamflow biases in both 2003 and 2004 are smoother than those of the rainfall inputs. This possibly is a result of the filtering effect of the runoff model as it converts highly variable rainfall input to streamflow. The significantly large rainfall bias in October of 2004 is translated to a smaller streamflow bias probably as the model became relatively dry and therefore did not convert the excess rainfall input into surface runoff. CMORPH-based streamflow in 2003 is mostly 0.25 to 0.5 times the gauge observations showing underestimation though this streamflow differences became much smaller in 2004. Overall, these differences were reduced when the bias-corrected CMORPH rainfall amounts served as model inputs. An exception is that TSF, which is obtained using a space-time constant correction factor, only slightly altered the streamflow bias. For most parts of the wet season, the streamflow bias significantly decreased when time variable bias correction is applied. Accounting for both spatial and temporal variation of the CMORPH bias factor further reduced the streamflow bias.

Figure 5. Streamflow bias (Q_{Bias}, Equation (9)) of streamflow simulations driven by different CMORPH rainfall inputs. Q_{Bias} was calculated using a moving window of past 7 days. Streamflow simulations driven by gauge observations served as the reference.

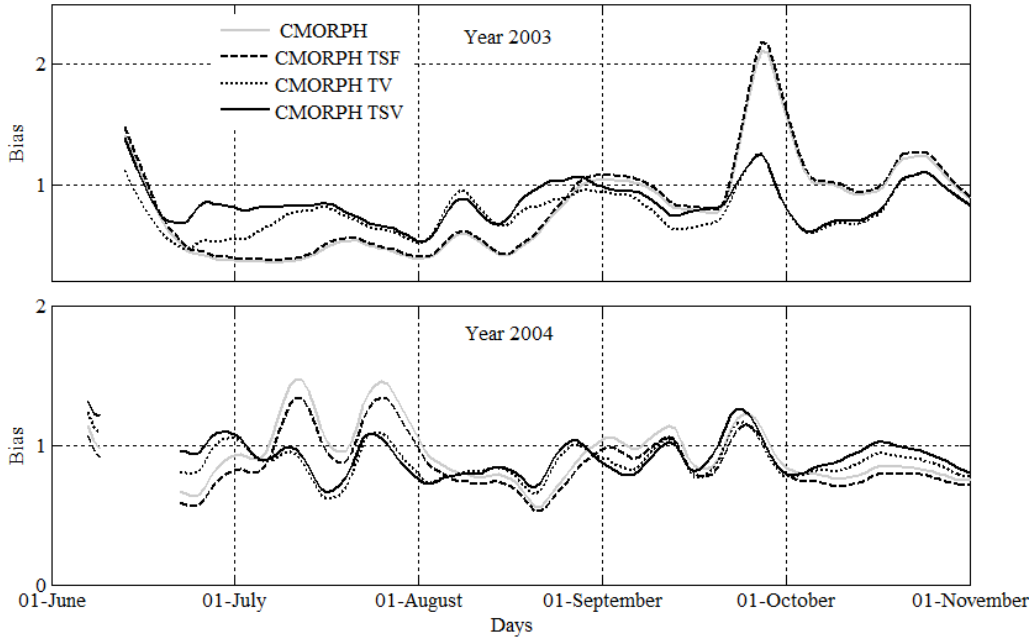

4. Conclusions

Various studies have indicated that satellite rainfall products are contaminated with systematic and random errors. However, not much has been done to illustrate how these products can be made applicable for various purposes by reducing their errors. In this study, the effect of rainfall bias correction in a high-resolution satellite-based product (CMORPH) on the performance of a rainfall-runoff model was assessed. The study is unique as we assess the importance of space and time aspects of CMORPH bias for rainfall-runoff modeling in a data scarce catchment. Our findings contribute to efforts that aim towards enhancing the real-world applicability of satellite rainfall products. The study site is the Gilgel Abbay catchment at the source of the Blue Nile in Eastern Africa—an example of many world regions that can benefit from satellite-based rainfall products for resource assessments and monitoring. Results and conclusions of the present study are summarized below.

CMORPH has large rainfall biases (−2.3 mm·d^{-1} on average and by up to ±30 mm·d^{-1}) with spatial as well as inter-annual and intra-annual variations in Gilgel Abbay catchment. Such biases could be related not only to rain generation mechanisms but also to the sampling and retrieval errors of satellite products [51]. We have showed through cross validation that it is not always the case that gauge-only, or satellite-only estimates, outperform one another. This suggests rainfall estimation can benefit from combined use of satellite and rain gauge data.

We applied three bias correction schemes to correct the bias CMORPH estimates. Space-time fixed, time variable and space-time variable bias factors were estimated to correct CMORPH estimates. One of the significant achievement of analysis indicated that the most important aspect of the CMORPH bias is its temporal variation as accounting for it substantially reduced the rainfall bias. In some instances, it was not possible to noticeably reduce the catchment-average bias. Particularly, absence of

gauges in the middle and south-east parts of the catchment is presumed to have contributed to the observed mismatches between bias-corrected CMORPH and gauge rainfall amounts.

An application of the HBV hydrologic model indicated that the model should be calibrated independently for satellite-only or satellite-gauge rainfall data in order to achieve high model performance. However, we observed that the calibration procedure compensated for rainfall input errors by changing the optimum values of model parameters as rainfall input changes. In particular, parameters that control the volume of the simulated hydrograph showed largest sensitivity to the different rainfall inputs. However, it was noted that the optimal parameter values stayed within the physically allowable ranges.

HBV better captured observed hydrograph patterns and volume when bias-corrected CMORPH estimates were used instead of the uncorrected estimates. We observed that the runoff model translates small rainfall errors to larger streamflow errors. The magnitudes of such error amplifications became smaller for bias-corrected satellite data than those for the satellite-only data. In the present study, −18% bias of CMORPH rainfall inputs is translated to −27% streamflow bias. The bias amplification was reduced (from −13% rainfall bias to only −17% streamflow bias) when space and time varying bias corrections were applied to the CMORPH rainfall input. Accounting for the temporal variability of CMORPH bias has the largest influence on model simulations and should be taken into account. The error propagation is found to depend, not only on errors in rainfall inputs, but also on the accumulated rainfall which affect the actual moisture and water storage in the model stores. Future studies should assess comparative advantages of various bias correction algorithms that account for the temporal aspects of bias and that received applications in climate change and radar rainfall studies. There is also a need to devote efforts towards operationalizing the bias correction algorithms.

Acknowledgment

Support for this study was provided by the National Science Foundation (NSF) through Award Number OISE-0914618 to the University of Louisiana at Lafayette, and by the the NASA EPSCoR/BoR DART2 program and the NASA Grant to Louisiana Space (LaSPACE) Consortium. Support provided by the University of Louisiana at Lafayette Computational and Visualization Enterprise (CAVE) Consortium is acknowledged. Support is also received from the CGIAR Research Program on Water, Land and Ecosystems (WLE), which is led by International Water Management Institute (IWMI)

Author Contributions

Emad Habib and Alemseged Tamiru Haile had the original idea for the study with all co-authors carried out the design. Alemseged Tamiru Habib was responsible for mentoring and follow-up of study participants. Alemseged Tamiru Haile and Nazmus Sazib were responsible for data preparation and all authors carried out the analyses. Alemseged Tamiru Haile, and Emad Habib drafted the manuscript, which was revised by Tom Rientjes, Yu Zhang, and the other authors. Tom Rientjes provided the modeling tools. All authors read and approved the final manuscript.

Conflicts of Interest

The authors declare no conflict of interest.

References

1. Haile, A.T.; Habib, E.; Rientjes, T.H.M. Evaluation of the Climate Prediction Center (CPC) morphing technique (CMORPH) rainfall product on hourly time scales over the source of the Blue Nile River. *Hydrol. Process.* **2013**, *27*, *1829–1839*.
2. Kondragunta, C.; Shrestha, K. Automated real-time operational rain gauge quality controls in NWS hydrologic operations. In Proceedings of the 20th AMS Conference on Hydrology, Atlanta, GA, USA, 29 January–2 February 2006.
3. AghaKouchak, A.; Mehran, A.; Norouzi, H.; Behrangi, A. Systematic and random error components in satellite precipitation data sets. *Geophys. Res. Lett.* **2012**, *39*, doi:10.1029/2012GL051592.
4. Dinku, T.; Ceccato, P.; Grover-Kopec, E.; Lemma, M.; Connor, S.J.; Ropelewski, C.F. Validation of satellite rainfall products over East Africa's complex topography. *Int. J. Remote Sens.* **2007**, *28*, 1503–1526.
5. Habib, E.; Haile, A.T.; Tian, Y.; Joyce, R. Evaluation of the high-resolution CMORPH satellite-rainfall product using dense rain gauge observations and radar-based estimates. *J. Hydrometeorol.* **2012**, *13*, 1784–1798.
6. Yilmaz, K.K.; Hogue, T.S.; Hsu, K.; Sorooshian, S.; Gupta, H.V.; Wagener, T. Intercomparison of rain gauge, radar, and satellite-based precipitation estimates with emphasis on hydrologic forecasting. *J. Hydrometeorol.* **2005**, *6*, 497–517.
7. Zhang, Y.; Seo, D-J.; Kitzmiller, D.; Lee, H.; Kuligowski, R.J.; Kim, D.; Kondragunta, C.R. Comparative strengths of SCaMPR satellite QPEs with and without TRMM ingest *vs.* gridded gauge-only analyses. *J. Hydrometeorol.* **2013**, *14*, 153–170.
8. Bitew, M.M.; Gebremichael, M. Assessment of satellite rainfall products for streamflow simulation in medium watersheds of the Ethiopian highlands. *Hydrol. Earth Syst. Sci.* **2011**, *15*, 1147–1155.
9. Bitew, M.M.; Gebremichael, M. Evaluation of satellite rainfall products through hydrologic simulation in a fully distributed hydrologic model. *Water Resour. Res.* **2011**, 47, doi:10.1029/2010WR009917.
10. Joyce, R.J.; Janowiak, J.E.; Arkin, P.A.; Xie, P.P. CMORPH: A method that produces global precipitation estimates from passive microwave and infrared data at high spatial and temporal resolution. *J. Hydrometeorol.* **2004**, *5*, 487–503.
11. Habib, E.; ElSaadani, M.; Haile, A.T. Climatology-focused evaluation of CMORPH and TMPA satellite rainfall products over the Nile Basin. *J. Appl. Meteorol. Climatol.* **2012**, *51*, 2105–2121.
12. Ebert, E.E.; Janowiak, J.E.; Kidd, C. Comparison of near-real-time rainfall estimates from satellite observations and numerical models. *Bull. Am. Meteorol. Soc.* **2007**, *88*, 47–64.
13. Pereira, F.A.J.; Carbone, R.E.; Janowiak, J.E.; Arkin, P.; Joyce, R.; Hallak, R.; Ramos, C.G.M. Satellite rainfall estimates over South America—Possible applicability to the water management of large watersheds. *J. Am. Water Resour. Assoc.* **2010**, *46*, 344–360.

14. Anagnostou, E.N.; Maggioni, V.; Nikolopoulos, E.I.; Meskele, T.; Hossain, F.; Papadopoulos, A. Benchmarking high-resolution global satellite rainfall products to radar and rain-gauge rainfall estimates. *IEEE Trans. Geosci. Remote. Sens.* **2010**, *48*, 1667–1683.
15. Sapiano, M.R.P.; Arkin, P.A. An Intercomparison and validation of high-resolution satellite precipitation estimates with 3-hourly gauge data. *J. Hydrometeorol.* **2009**, *10*, 149–166.
16. Smith, T.M.; Arkin, P.A.; Bates, J.J.; Huffman, G.J. Estimating bias of satellite-based precipitation estimates. *J. Hydrometeorol.* **2006**, *7*, 841–856.
17. CMORPH Improvements: A Kalman Filter Approach to Blend Various Satellite Rainfall Estimate Inputs and Rain Gauge Data Integration. Available online: http://adsabs.harvard.edu/abs/2009 EGUGA..11.9810J (accessed on 25 September 2013).
18. Joyce, R.J.; Xie, P.; Janowiak, J.E. Kalman filter based CMORPH. *J. Hydrometeorol.* **2011**, *12*, 1547–1563.
19. Seo, D.-J.; Breidenbach, J. Real-time correction of spatially nonuniform bias in radar rainfall data using rain gauge measurements. *J. Hydrometeorol.* **2002**, *3*, 93–111.
20. Seo, D.-J.; Briedenbach, J.P.; Johnson, E.R. Real-time estimation of mean field bias in radar rainfall data. *J. Hydrol.* **1999**, *223*, 131–147.
21. Zhang, J.; NOAA/NSSL; Norman, O.K.; Howard, K.; Vasiloff, S.; Langston, C.; Kaney, B.; Arthur, A.; van Cooten, S.; Kelleher, K.; *et al.* National Mosaic and QPE (NMQ) system—Description, results and future plan. In Proceedings of the 34th Conference on Radar Meteor, Williamsburg, VA, USA, 6 October 2009.
22. Huffman, G.J.; Adler, R.F.; Bolvin, D.T.; Gu, G.J.; Nelkin, E.J.; Bowman, K.P.; Hong, Y.; Stocker, E.F.; Wolff, D.B. The TRMM multisatellite precipitation analysis (TMPA).Quasi-global, multiyear, combined-sensor precipitation estimates at fine scales. *J. Hydrometeorol.* **2007**, *8*, 38–55.
23. Boushaki, F.I.; Hsu, K.-L.; Sorooshian, S.; Park, G.-H.; Mahani, S.; Shi, W. Bias adjustment of satellite precipitation estimation using ground-based measurement: A case study evaluation over the southwestern United States. *J. Hydrometeorol.* **2009**, *10*, 1231–1242.
24. Li, M.; Shao, Q. An improved statistical approach to merge satellite rainfall estimates and raingauge data. *J. Hydrol.* **2010**, *385*, 51–64.
25. Vila, D.A.; de Goncalves, L.G.G.; Toll, D.L.; Rozante, J. Statistical evaluation of combined daily gauge observations and rainfall satellite estimates over continental South America. *J. Hydrometeorol.* **2009**, *10*, 533–543.
26. Hong, Y.; Hsu, K.; Moradkhani, H.; Sorooshian, S. Uncertainty quantification of satellite precipitation estimation and Monte Carlo assessment of the error propagation into hydrologic response. *Water Resour. Res.* **2006**, *42*, doi:10.1029/2005WR004398.
27. Chiang, Y.-M.; Hsu, K.-L.; Chang, F.-J.; Hong, Y.; Sorooshian, S. Merging multiple precipitation sources for flash flood forecasting. *J. Hydrol.* **2007**, *340*, 183–196.
28. Tobin, K.J.; Bennett, M.E. Adjusting satellite precipitation data to facilitate hydrologic modeling. *J. Hydrometeorol.* **2010**, *11*, 966–978.
29. Tian, Y.; Peters-Lidard, C.D.; Eylander, J.B. Real-time bias reduction for satellite-based precipitation estimates. *J. Hydrometeorol.* **2010**, *11*, 1275–1285.

30. Krakauer, N.Y.; Pradhanang, S.M.; Lakhankar, T.; Jha, A.K. Evaluating satellite products for precipitation estimation in mountain regions: A case study for Nepal. *Remote Sens.* **2013**, *5*, 4107–4123.
31. Artan, G.; Gadain, H.; Smith, J.L.; Asante, K.; Bandaragoda, C.J.; Verdin, J.P. Adequacy of satellite derived rainfall data for stream flow modeling. *Nat. Hazards* **2007**, *43*, 167–185.
32. Zeweldi, D.A.; Gebremichael, M.; Downer, C.W. On CMORPH rainfall for stream flow simulation in a small, Hortonian watershed. *J. Hydrometeorol.* **2011**, *12*, 456–466.
33. Behrangi, A.; Khakbaz, B.; Jaw, T.C.; AghaKouchak, A.; Hsu, K.; Sorooshian, S. Hydrologic evaluation of satellite precipitation products over a mid-size basin. *J. Hydrol.* **2011**, *397*, 225–237.
34. Yong, B.; Ren, L.-L.; Hong, Y.; Wang, J.-H.; Gourley, J.J.; Jiang, S.-H.; Chen, X.; Wang, W. Hydrologic evaluation of Multisatellite Precipitation Analysis standard precipitation products in basins beyond its inclined latitude band: A case study in Laohahe basin, China. *Water Resour. Res.* **2010**, *46*, doi:10.1029/2009WR008965.
35. Sorooshian, S.; AghaKouchak, A.; Arkin, P.; Eylander, J.; Foufoula-Georgiou, E.; Harmon, R.; Hendrickx, J.; Imam, B.; Kuligowski, R.; Skahill, B.; *et al*. Advanced concepts of remote sensing of precipitation at multiple scales. *Bull. Am. Meteorol. Soc.* **2011**, 92, 1353–1357.
36. Gebremichael, M.; Anagnostou, E.N.; Bitew, M. Critical steps for continuing advancement of satellite rainfall applications for surface hydrology in the Nile River basin. *J. Am. Water Resour. Assoc.* **2010**, *46*, 361–366.
37. Rientjes, T.H.M.; Perera, B.U.J.; Haile, A.T.; Reggiani, P.; Muthuwatta, L.P. Regionalisation for lake level simulation—The case of Lake Tana in the Upper Blue Nile, Ethiopia. *Hydrol. Earth Syst. Sci.* **2011**, *15*, 1167–1183.
38. Haile, A.T.; Rientjes, T.H.M.; Gieske, A.S.M.; Gebremichael, M. Rainfall variability over mountainous and adjacent lake areas: The case of Lake Tana basin at the source of the Blue Nile River. *J. Appl. Meteorol. Climatol.* **2009**, *48*, 1696–1717.
39. Rientjes, T.H.M.; Haile, A.T.; Ayele, A.F. Diurnal rainfall variability over the Upper Blue Nile: A remote sensing based approach. *Int. J. Appl. Earth Obs. Geoinf.* **2013**, *21*, 311–325
40. Haile, A.T.; Rientjes, T.H.M.; Habib, E.; Jetten, V.; Gebremichael, M. Rain event properties at the source of the Blue Nile River. *Hydrol. Earth Syst. Sci.* **2011**, *15*, 1023–1034.
41. Abdo, K.S.; Fiseha, B.M.; Rientjes, T.H.M.; Gieske, A.S.M.; Haile, A.T. Assessment of climate change impacts on the hydrology of Gilgel Abbay catchment in Lake Tana basin, Ethiopia. *Hydrol. Process.* **2009**, *23*, 3661–3669.
42. Rientjes, T.H.M.; Haile, A.T.; Mannaerts, C.M.M.; Kebede, E.; Habib, E. Changes in land cover and stream flows in Gilgel Abbay catchment, Upper Blue Nile basin—Ethiopia. *Hydrol. Earth Syst. Sci. Discuss.* **2011**, *7*, 9567–9598.
43. Wale, A.; Rientjes, T.H.M.; Gieske, A.S.M.; Getachew, H.A. Ungauged catchment contributions to Lake Tana's water balance. *Hydrol. Process.* **2009**, *23*, 3682–3693.
44. Allen, R.G.; Pereira, L.S.; Raes, D.; Smith, M. *Crop Evapotranspiration: Guidelines for Computing Crop Water Requirements*; Irrigation and Drainage Paper; United Nations Food and Agriculture Organization: Rome, Italy, 1998; p. 300.

45. Lindström, G.; Johansson, B.; Persson, M.; Gardelin, M.; Bergström, S. Development and test of the distributed HBV-96 hydrological model. *J. Hydrol.* **1997**, *201*, 272–288.
46. Booij, M.J. Impact of climate change on river flooding assessed with different spatial model resolutions. *J. Hydrol.* **2005**, *303*, 176–198.
47. Deckers, D.L.E.H.; Booij, M.J.; Rientjes, T.H.M.; Krol, M.S. Catchment variability and parameter estimation in multi-objective regionalisation of a rainfall-runoff model. *Water Resour. Manag.* **2010**, *24*, 3961–3985.
48. Merz, R.; Blöschl, G. Regionalisation of catchment model parameters. *J. Hydrol.* **2004**, *287*, 95–123.
49. Rientjes, T.H.M.; Muthuwatta, L.P.; Bos, M.G.; Booij, M.J.; Bhatti, H.A. Multi-variable calibration of a semi-distributed hydrological model using streamflow data and satellite based evapotranspiration. *J. Hydrol.* **2013**, *505*, 276–290.
50. Seibert, J. Estimation of parameter uncertainty in the HBV model. *Nord. Hydrol.* **1997**, *28*, 4–5.
51. Gebremichael, M.; Krajewski, W.F. Characterization of the temporal sampling error inspace-time-averaged rainfall estimates from satellites. *J. Geophys. Res.* **2004**, *109*, doi:10.1029/2004JD004509.